Open Access Full Text Article

Synthesis and application of ZnO/rGo-based magnetic nanocomposite materials for treatment of organic pigments

Nguyen Khac Duy[1], Nguyen Van Thanh[2], Doan Thi Tram[2], Phạm Van Tuan[2], Nguyen Thanh Tuan[2], Pham Ngoc Anh[3], Uong Thi Ngoc Ha[4], Bui Thi Le Thuy[1,*]

ABSTRACT

Photocatalysis is one of the most effective techniques for treating organic pigments in wastewater. Some composite materials are prepared by combining photocatalysts and magnetic adsorbents and are used for treating organic pigments in water. In this work, zinc oxide-doped rGO-based nanocomposite materials were prepared via a simple process. In particular, Fe_2O_3 was added to those nanocomposites to form magnetic photocatalytic materials that can be recovered and reused after reactions. The material structure was characterized by scanning electron microscopy (SEM), Fourier transform infrared (FT-IR) spectroscopy, and ultraviolet–visible diffuse reflectance spectroscopy (UV–Vis DRS). Rhodamine B (RhB) and methylene blue (MB) were photochemically treated with the prepared magnetic photocatalytic materials. Ultraviolet–visible spectroscopy (UV–Vis) was used to determine the concentrations of organic pigments before and after treatment with the materials. The photocatalytic degradation efficiency of MB and RhB reached more than 84% after 75 min and more than 98% after 6 h, respectively. The magnetic photocatalytic materials effectively recovered (up to 92%) after 3 cycles. In addition, the mechanism of photocatalytic degradation was investigated via capture experiments. The results indicated that magnetic photocatalytic materials can effectively treat MB and RhB in water and can be recovered and reused, showing their potential as attractive alternatives to treating organic pigments in wastewater.

Key words: nanocomposite, magnetic, photocatalysis, organic pigment treatment

[1]*Key research group: Green Chemistry Process (HUMG-GCP), Ha noi University of Mining and Geology, 18 Vien, Duc Thang yard, Bac Tu Liem district, Ha Noi.*

[2]*Ha noi University of Mining and Geology, 18 Vien, Duc Thangyard, Bac Tu Liem district, Ha Noi.*

[3]*Dong Da High School, 10, Quan Tho 1, Ton Duc Thang, Hang Bọt yard, Dong Da district, Ha Noi*

[4]*Hong Bang University, 215 Dien Bien Phu, 15 yard, Binh Thanh district, Ho Chi Minh City*

Correspondence

Bui Thi Le Thuy, Key research group: Green Chemistry Process (HUMG-GCP), Ha noi University of Mining and Geology, 18 Vien, Duc Thang yard, Bac Tu Liem district, Ha Noi.

Email: thuykhai2001@gmail.com

Check for updates

VNUHCM PRESS

INTRODUCTION

In recent years, the textile and dyeing industry has significantly developed and greatly contributed to the overall economic development of the country. However, the problem of environmental pollution arising from the production process has also increased. The textile and dyeing industries release large amounts of wastewater with high concentrations of pollutants into the environment every year. In addition, some wastewater treatment systems in developing countries have not been invested in, or the damaged system has not been promptly repaired. These factors could significantly impact the underwater ecosystem and especially cause a serious shortage of clean water. Wastewater treatment, especially for textile wastewater, has become highly important and urgent. Many studies have focused on treating wastewater and improving water quality. Currently, many methods are used to treat textile wastewater, such as mechanical methods, chemical methods, chemical–physical methods, and biological methods.

The photodegradation method uses photoactive catalysts to decompose toxic components in textile and dyeing industry wastewater. This method, which has high treatment efficiency and low cost, is promising for treating textile wastewater. Maksoud et al.[1] gathered more than 400 reports on research projects using magnetic materials to treat toxic components in wastewater. In those studies, magnetic materials were also functionalized and coated on inorganic or organic materials such as polymers and chitosan to increase efficiency[2]. However, these studies have focused on pollutants separately, not on the simultaneous treatment of pollutants, while any type of wastewater contains many different types of pollutants. Zinc oxide (ZnO) is a promising n-type semiconductor material used in many applications, such as solar cells[3], antibacterial surface coatings[4], light-emitting diodes (LEDs), nanoelectricity generators, and photocatalytic applications[5]. ZnO nanostructures have high chemical, optical and electrical conductivity stability. When ZnO is used as a photocatalyst, electron–hole pairs that are photogenerated when excited can react with oxygen and water molecules to create free radicals that can decompose organic and inorganic compounds in the aquatic environment. Sonu Kumar et al.[6] covered ZnO nanomaterials with rGO (ZnO/rGO) as a photocatalyst to de-

compose 4-bromophenol (4-BP) and diethyl phthalate (DEP). These are persistent organic pollutants in wastewater (mainly aromatic compounds). The results show that the ZnO/rGO nanomaterials can decompose more than 95% of the 4-BP and DEP. However, the recovery ability of the material has not been evaluated. Juan Xie et al. prepared Fe_2O_3/ZnO materials capable of treating pentachlorophenol with an efficiency greater than 95% after 4 hours under UV light conditions. The material shows positive recovery[6]. Research by Sujoy Kumar Mandal et al. revealed that the use of ZnO quantum dots/rGO to treat MB and Rhodamine 6G (2019) has a high dye degradation efficiency under UV irradiation.[7] One method for synthesizing materials is the hydrothermal method. Zhuang Liu et al. (2020) researched the synthesis of Fe_2O_3/rGO using different hydrothermal methods as anode materials for lithium-ion batteries.[8] Sugianto Sugiantoa et al. (2023) researched the hydrothermal synthesis of GO/ZnO composites and their micromorphology and electrochemical performance.[9] These studies all successfully synthesized the materials via a hydrothermal method.

In this article, we describe a method to prepare new nanocomposite materials for treating organic pigments in water. This involves the combination of photocatalytic (ZnO, rGO) and magnetic active (Fe_2O_3) ingredients in Fe_2O_3/ZnO/rGO nanocomposite materials. Our goal was to develop a material with simultaneous photocatalytic and magnetic activities for treating MB and RhB in wastewater. The material can be easily recovered and reused, the procedure of wastewater treatment becomes simple, and its cost is reduced.

The organization of this paper is as follows:

In the experimental section, we described (i) the preparation and characterization of the Fe_2O_3, rGO, and Fe_2O_3/ZnO/rGO $_{materials}$ used in this study; (ii) the methods used for the treatment of MB and RhB via prepared Fe_2O_3/ZnO/rGO; and (iii) the recovery and reuse of the Fe_2O_3/ZnO/rGO material after MB and RhB treatment.

In the results section, we present the results of the preparation of Fe_2O_3, rGO, and Fe_2O_3/ZnO/rGO and their characterization via FT-IR, SEM, and UV–Vis DRS. In this section, we also present the results of the treatment of MB and RhB in aqueous solution and the recovery and reusability of spent Fe_2O_3/ZnO/rGO by the application of a magnetic field.

In the discussion section, we discuss the results of the preparation and characterization of the Fe_2O_3,

rGO, and Fe_2O_3/ZnO/rGO materials and the results of the MB and RhB treatments. We propose a mechanism for the photodegradation of MB and RhB. Finally, the possibility of recovering and reusing Fe_2O_3/ZnO/rGO is mentioned.

EXPERIMENTAL

Chemicals

Zinc acetate dihydrate 99%, iron(III) nitrate nonahydrate 99%, hydrogen peroxide 30%, hydrochloric acid 35%, sulfuric acid 98%, sodium hydroxide 99%, ethanol 99%, potassium permanganate 99%, methylene blue, acetic acid 99% and acetone 99% were supplied by Xilong Company; ascorbic acid 99% (Fisher), graphite (Merck), ammonia solution 25% (GHTech), and Rhodamine B (Oxford Lab Fine Chem LLP) were used without further purification. Distilled water was obtained from the laboratory of Hanoi University of Mining and Geology.

Preparation of nanocomposite materials
Preparation of Fe_2O_3

First, 20 g of $Fe(NO_3)_3 \cdot 9H2O$ and 100 mL of ethanol were added to a round-bottom flask, and the mixture was stirred to obtain a homogeneous phase. Then, 10 mL of acetic acid was added, followed by slowly adding 60 mL of ammonia solution into the flask while stirring at room temperature (25°C). The mixture was refluxed for 1 hour at 180°C. After the reaction, the excess NH_3 was evaporated under vacuum for 2–3 hours. The remaining mixture was filtered, and the resulting solid was washed with distilled water and ultrasonicated for 30 minutes. The water was then evaporated, and the solid was heated at 400°C for 3 hours. A dark brown Fe_2O_3 solid was obtained.

Preparation of GO[10,11]

The procedure followed the method of Bui et al.[10,11] with a minor modification. First, 2.5 g of $NaNO_3$ and 5 g of graphite were slowly added to $_{115\ mL\ of}$ 98% H2SO4 solution, which was maintained at 3–5°C. Stirring with a magnetic stirrer was continued for 30 min, and then 15 g of $KMnO_4$ was gradually added while the temperature was maintained below 15°C. The temperature of the reaction mixture was increased to 35°C, and the mixture was stirred for approximately 30 min; then, distilled water was gradually introduced into the reaction mixture to maintain the temperature at approximately 45°C. The temperature was subsequently increased to 95°C, and the reaction mixture was stirred for an additional 15 min

at this temperature. Next, the temperature of the system was reduced slowly to room temperature, 50 mL of H_2O_2 solution was added to the mixture, and the mixture was stirred for 20 minutes. The solid of the final mixture was centrifuged at 8000 rpm for 6 min to obtain GO. Then, the GO was dispersed in a 0.1 M HCl solution, stirred for 15 min and centrifuged to purify the GO from the impurities. After drying at 70°C - 80°C and grinding with a ceramic mortar, the resulting product was GO.

Preparation of rGO[10,11]

The procedure follows the method of Bui et al.[10,11] with some modifications, and the details are as follows. First, 10 g of arcic acid was dissolved in 100 ml of distilled water. One gram of GO was dispersed in 100 ml of distilled water by stirring and ultrasonication for one hour to form a suspension. Then, 3 grams of gelatin was gradually introduced, and the temperature was increased to 70°C. One hundred milliliters of aqueous solution containing 10 g of ascorbic acid was added slowly to the suspension within 2 hours. The mixture was subsequently heated at 70°C for 12 hours. The resulting mixture was centrifuged and filtered, washed with water and ethanol, and dried at 60°C. The obtained product was reduced graphene oxide (rGO).

Preparation of ZnO/rGO

A total of 0.5 g of rGO was introduced into a beaker containing 100 mL of distilled water, after which the mixture was sonicated for 30 minutes. First, 2.75 g of zinc acetate dihydrate ($Zn(CH_3COO)_2\cdot2H_2O$) was dissolved in 50 mL of water and then stirred for 30 minutes. Two hundred milliliters of a solution containing 4 g of NaOH was slowly added to the zinc acetate solution, and a white milky precipitate appeared in the resulting mixture. The mixture was subsequently poured into a beaker containing rGO in water. The resulting mixture was refluxed for 36 hours at 180°C. The obtained mixture was filtered to collect the solid, which was washed several times with distilled water until the wash water was clear and the pH was neutral. The solid was dried at 70°C for 8 hours to obtain ZnO/rGO.

Preparation of Fe$_2$O$_3$/ZnO/rGO

First, 0.5 g of Fe_2O_3 was added to a beaker containing 60 mL of ethanol, and the mixture was stirred for 30 minutes. Then, 0.5 g of ZnO/rGO was added, and the mixture was stirred for 1 hour. After that, the mixture was sonicated for 30 minutes. Finally, the solvent was evaporated at 80°C for 1 h and turned dark brown to obtain the fine powder Fe_2O_3/ZnO/rGO.

Characterization

The structure of the solid materials was characterized via SEM (Hitachi S-4800), UV–Vis DRS (GBC Instrument-2885), and FT–IR (Jasco FT–IR-6800). The concentration of the dyes RhB or MB in the solution was determined via UV–Vis spectroscopy (Jasco V-750).

Evaluation of the photocatalytic activity of the materials

First, 0.05 g of the solid material was added to a beaker containing 50 mL of an aqueous solution with a concentration of 50 ppm MB or RhB dye. The MB (RhB) decomposition reaction occurred at 25°C and pH 8.0. The mixture was gently stirred in the dark for 30 minutes. Then, the reaction mixture was illuminated in a glass beaker with an 11 W compact lamp, and samples were taken at regular intervals, typically 1.5 to 2 mL each time, for UV–Vis measurement. The process was continued until the color of the solution clearly decreased. Finally, the solid material was collected after the treatment. The solid material after the first treatment process is used to start the second treatment process. This process was performed three times to determine the reusability and organic pigment degradation efficiency of this material.

RESULTS

Characterization results of the materials

Characterization of the Fe$_2$O$_3$ material

Figure 1 shows that the FT-IR spectrum of the Fe_2O_3 nanoparticles can be used to identify chemical bonds as well as functional groups.

The peak at 3414 cm^{-1} is characteristic of the stretching vibration of the OH group. The peak at 1636 cm^{-1} indicates the presence of C=O bonds. The intense peak at 570 cm^{-1} represents the Fe-O bond, which is characteristic of Fe_2O_3 [12]. The peak at 1636 cm-1 corresponds to the C=O bond of the residual COO group. However, the peak intensity is weak, meaning that the residual amount is very small. The COO functional group appears because acetic acid is used in the synthesis of the material.

SEM measurements (Figure 2) revealed that the Fe_2O_3 particles were very small, uniform, and spherical in shape. The image shows that iron nanoparticles are formed with sizes ranging from 30 nm to 50 nm.

Characterization of the GO and rGO materials

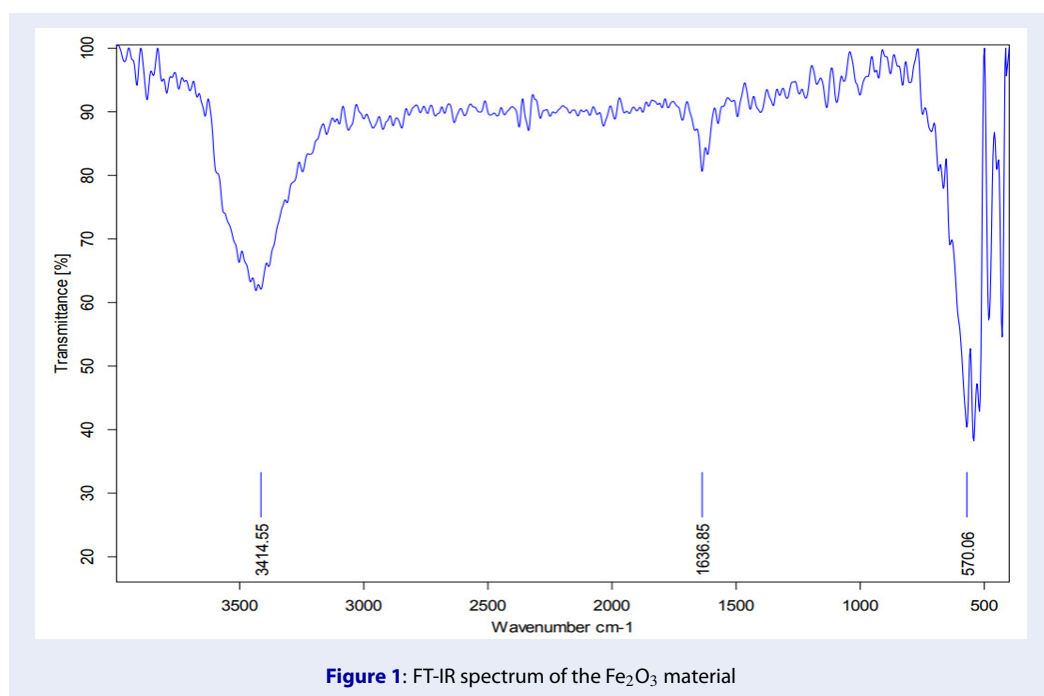The SEM images of GO and rGO are presented in Figures 3 and 4. The graphite surface has been separated
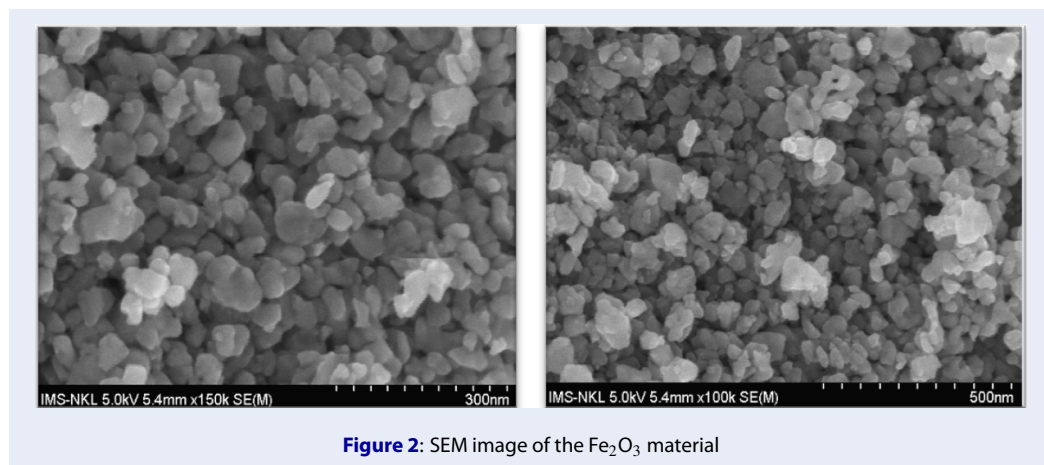
Figure 1: FT-IR spectrum of the Fe$_2$O$_3$ material

Figure 2: SEM image of the Fe$_2$O$_3$ material

into thinner layers at different magnifications. The GO surface is relatively uniform, indicating that the graphite surface has been oxidized. The SEM images also show that the graphite has been exfoliated after oxidation in a concentrated acidic medium.

The FT-IR measurement results of GO are shown in Figure 5. The peak at 3358 cm^{-1} is attributed to the presence of the OH functional group. The peak at 1714 cm^{-1} is characteristic of the C=O vibration, 1616 cm^{-1} corresponds to the C=C vibration, 1367 cm^{-1} indicates the presence of the C-OH group, and 1217 cm^{-1} and 1041 cm^{-1} are characteristic of the C-O vibration (alkoxy, epoxy)[13]. These results indicate the presence of oxygen-containing functional groups in GO.

The FT-IR measurement results of rGO are shown in Figure 6. The FT-IR results indicate that the vibrational frequencies of the oxygen-containing functional groups of GO are almost absent in the rGO samples. The intensity of the peaks has decreased. This is a result of the reduction process of the oxygen-containing functional groups on GO using ascorbic acid. These results are confirmed by the elimination and reduction in peak intensities, as shown in Figure 5.

The peak intensities at 3358 cm^{-1}, 1616 cm^{-1}, and 1217 cm^{-1} considerably decreased, and the peaks at 1367 cm^{-1} and 1041 cm^{-1} were no longer present.
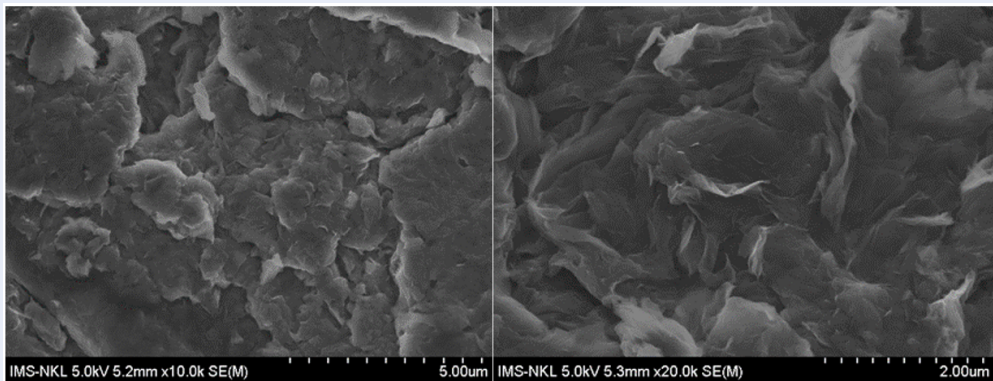
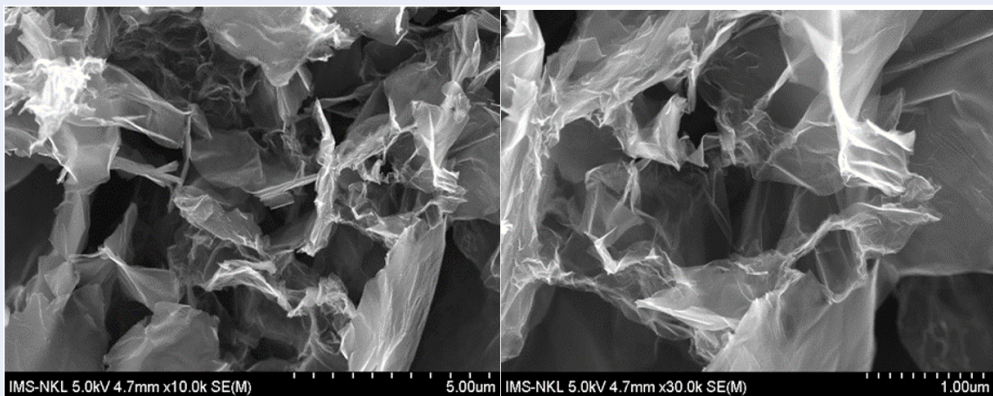**Figure 3**: SEM image of the GO material
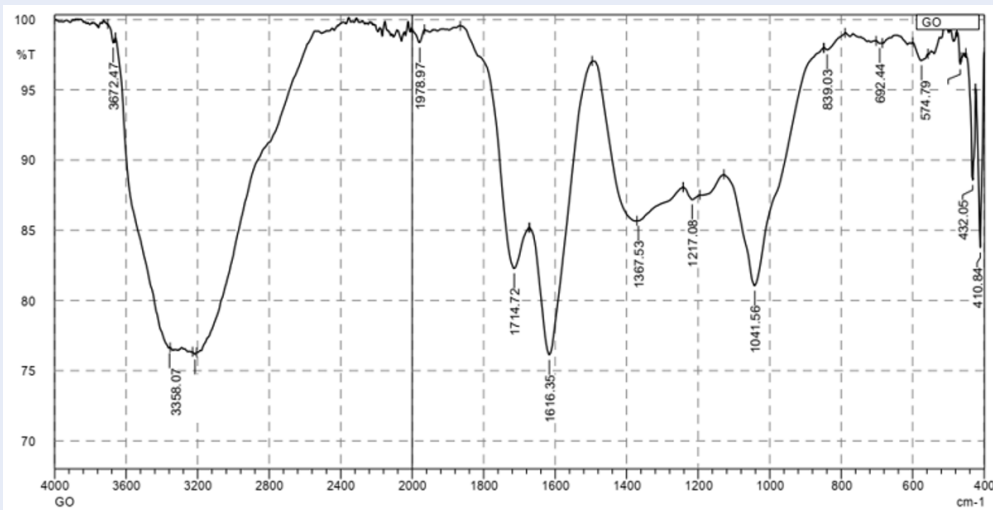

Figure 4: SEM image of the rGO material

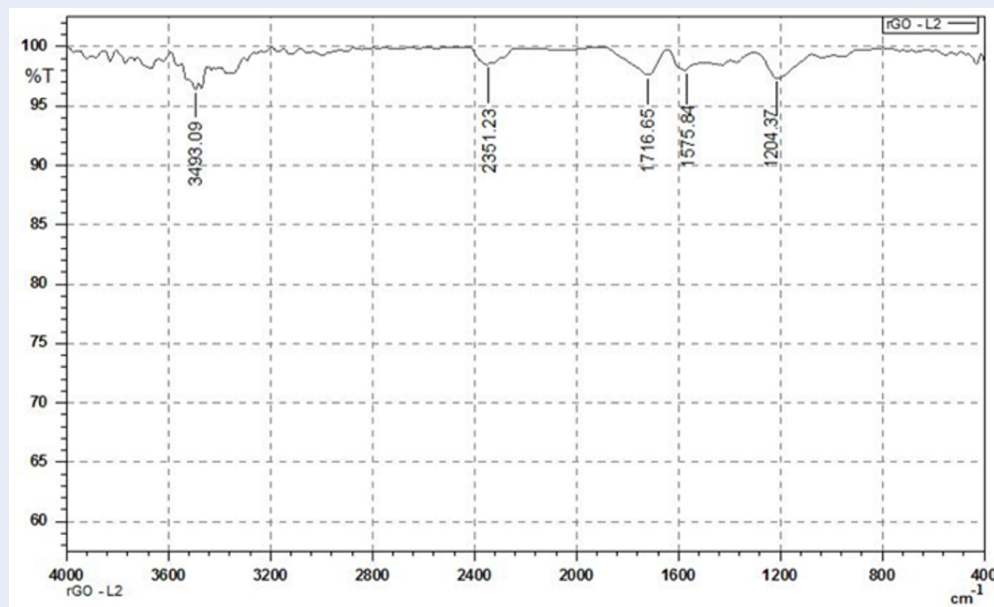**Figure 5**: FT-IR measurement results of the GO material

Figure 6: FT-IR measurement results of the rGO material.

This indicates that the number of oxygen-containing functional groups in GO has decreased. The FT-IR measurement results of rGO also confirm that although most of the oxygen-containing functional groups in GO have been reduced, some residual oxygenated functional groups are still present on the surface of rGO but with weaker intensities after reduction.

Characterization of the ZnO/rGO and Fe$_2$O$_3$/ZnO/rGO materials

The SEM images of ZnO/rGO and Fe$_2$O$_3$/ZnO/rGO are shown in Figures 7 and 8, indicating that ZnO and Fe$_2$O$_3$ were dispersed on the surface of the graphene sheets. The nearly spherical ZnO and Fe$_2$O$_3$ nanoparticles are randomly dispersed on the surface of the graphene. The formation of spherical ZnO nanoparticles may be attributed to the addition of OH-(NaOH), which accelerates the reaction rate, leading to the formation of more particles in a shorter time[14]. The graphene sheets are not perfectly flat but rather exhibit numerous folds. Therefore, the structures of ZnO and rGO are sometimes uneven.

The XRD spectra of the ZnO/rGO and Fe$_2$O$_3$/ZnO/rGO materials are shown in Figure 9 and Figure 10, respectively. The characteristic peaks for ZnO in Figure 9 were the peaks at 31.8°, 34.5°, 36.3°, 47.6°, 56.7°, 63.0°, and 68.0° 69.2°. The characteristic peaks for Fe$_2$O$_3$ in Figure 10 were the peaks at 24.2°, 33.2°, 35.7°, 40.9°, 49.5°, 54.1°, 62.6°, and 64.1°.

According to the EDX results of the Fe$_2$O$_3$/ZnO/rGO material in Figure 11, the C, Fe and Zn contents are 19.99%, 14.58% and 18.28%, respectively. The phase forms of Fe$_2$O$_3$ and ZnO are hematite-rhombohedral structures and zincite-hexagonal crystal structures, respectively. The XRD and EDX results above indicate that the ZnO/rGO and Fe$_2$O$_3$/ZnO/rGO materials were successfully synthesized.

Ultraviolet−visible diffuse reflectance spectroscopy (UV−Vis DRS) has been used to study the optical properties of photocatalysts. The UV−Vis DRS measurement results for determining the band gap energy of the synthesized materials are presented in Figure 12.

Fe$_2$O$_3$/ZnO/rGO has a high treatment ability in the visible light region, demonstrating the ability to capture visible light. An increase in the visible light absorption of Fe$_2$O$_3$/ZnO/rGO nanomaterials has been proposed because of the resonance effect between ZnO and rGO.[14] The bandgap energy of semiconductor-based photocatalytic materials plays a decisive role in the photocatalytic activity of the material. The range of photon energies for visible light is 1.7 to 3.3 eV. The bandgap energy of Fe$_2$O$_3$/ZnO/rGO = 2.85 eV (<3.3 eV). Therefore, photocatalytic activity is activated when compact lamps (in the visible light region) are used because there is still enough energy to activate the electron from the valence band (VB) to
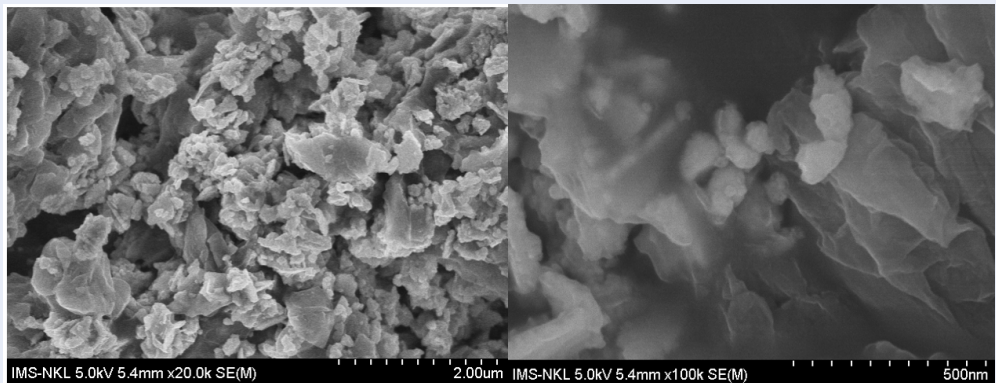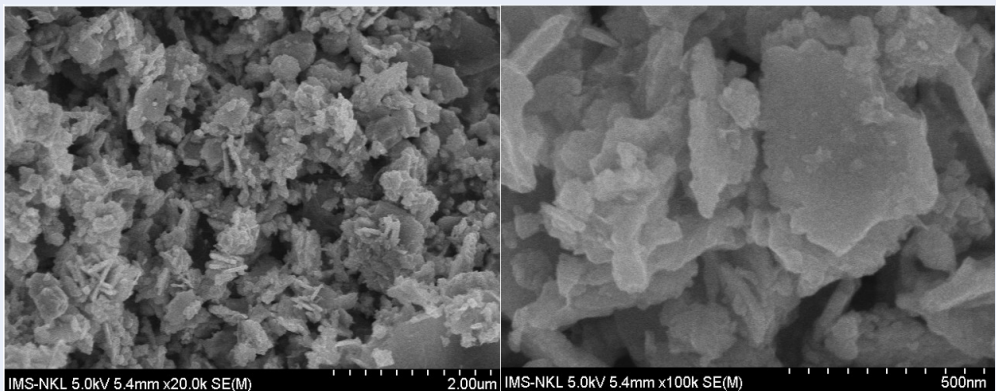
Figure 7: SEM image of the ZnO/rGO material.

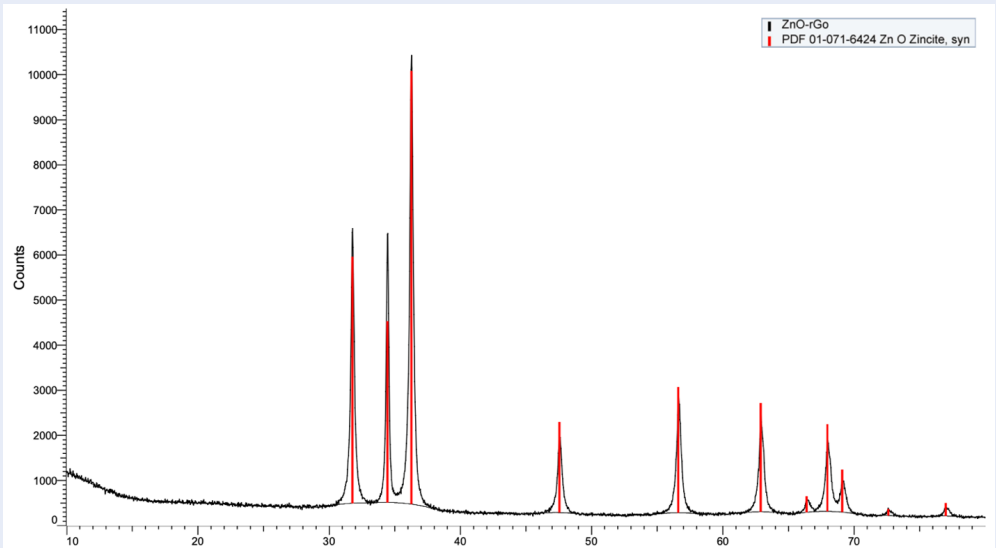**Figure 8**: SEM image of the Fe$_2$O$_3$/ZnO/rGO material

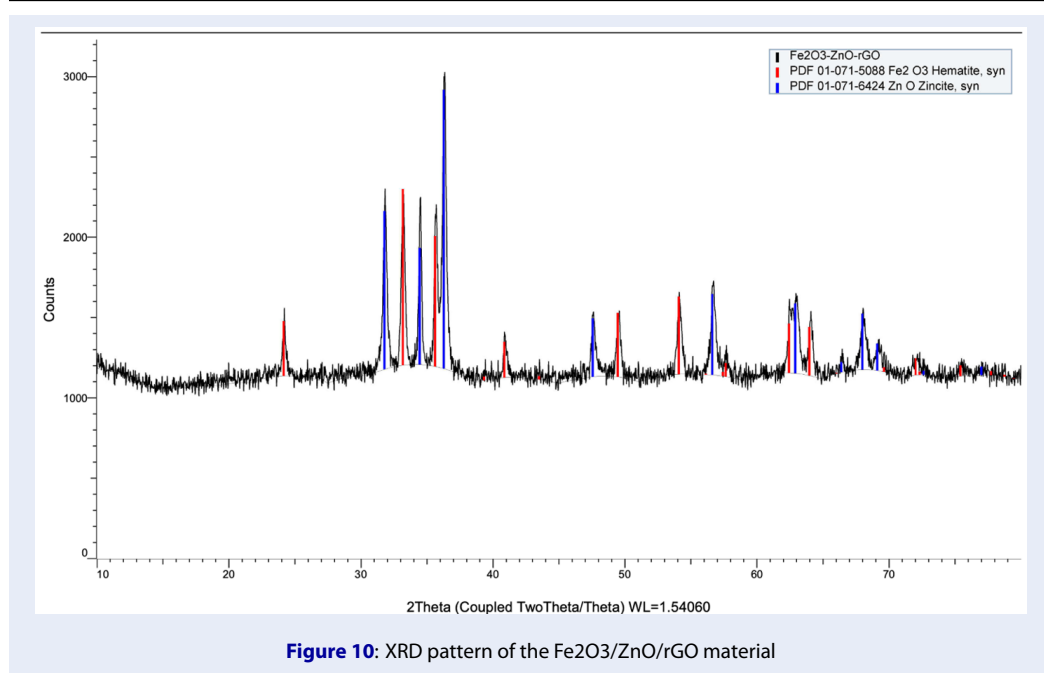**Figure 9**: XRD pattern of the ZnO/rGO material.

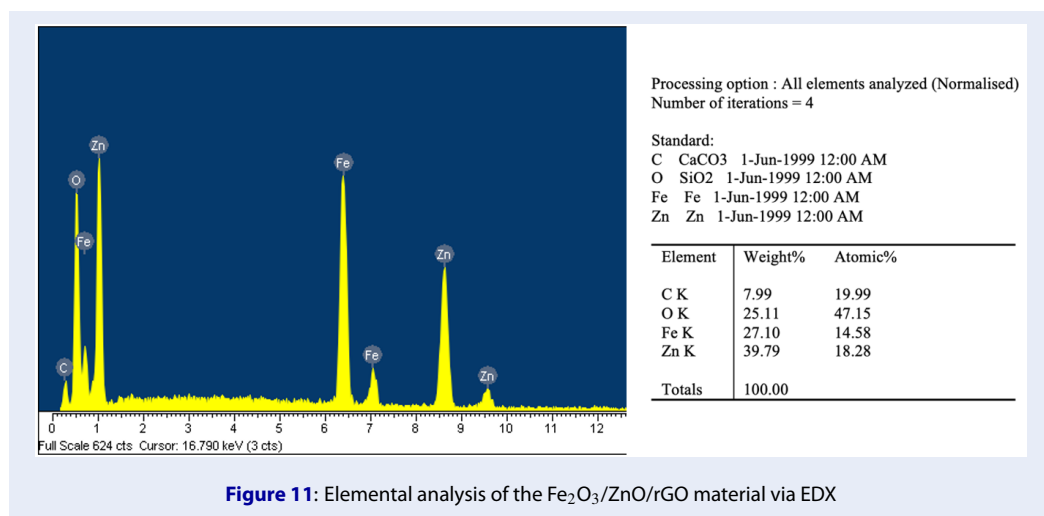**Figure 10**: XRD pattern of the Fe2O3/ZnO/rGO material

Figure 11: Elemental analysis of the Fe$_2$O$_3$/ZnO/rGO material via EDX

the conduction band (CB). The photocatalytic activity is still activated.

Evaluation of the photocatalytic activity for dye treatment

Treatment with methylene blue

Three materials, rGO, ZnO/rGO and Fe$_2$O$_3$/ZnO/rGO, are used for the treatment of MB in water, and the results are shown in Figure 13. During the first 30 min in the dark (not illuminated), the UV−VIS measurement results revealed that the MB concentration gradually decreased due to adsorption by the material. Without illumination, the MB concentration in the sample in contact with rGO decreased faster than that in contact with ZnO/rGO vs. Fe$_2$O$_3$/ZnO/rGO. However, the decrease in the MB concentration in the sample in contact with rGO slowed during the illumination period. ZnO/rGO and Fe$_2$O$_3$/ZnO/rGO can treat 84.8% of the material in 75 minutes.

The results of the rhodamine B

Rhodamine B treatment of three materials, rGO, ZnO/rGO and Fe$_2$O$_3$/ZnO/rGO, are shown in Figure 14.
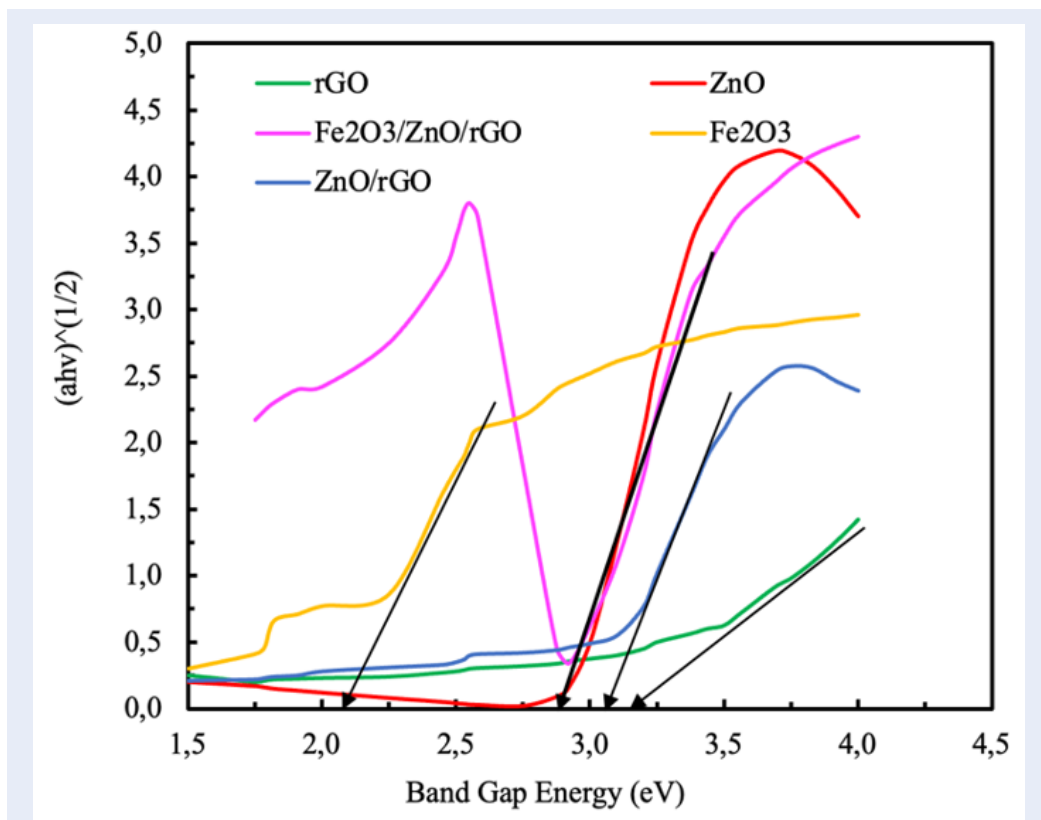
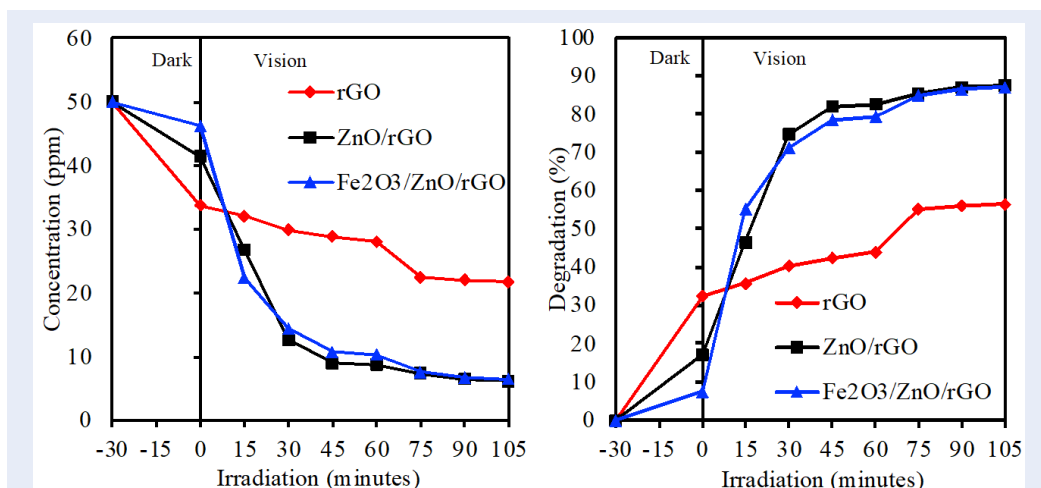**Figure 12**: UV–Vis DRS measurement results of the synthesized materials

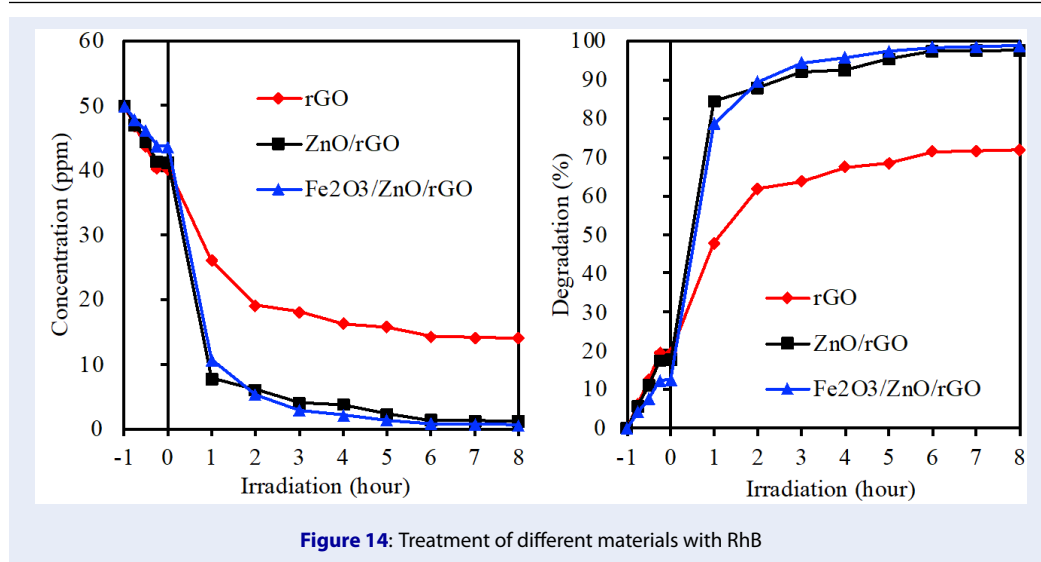**Figure 13**: Treaming of MB by different materials

Figure 14: Treatment of different materials with RhB

During the first hour in the dark, the UV–VIS measurement results revealed that the MB concentration gradually decreased due to adsorption by the material. Treatment of RhB with the ZnO/rGO and Fe_2O_3/ZnO/rGO samples reached 97.3% and 98.3%, respectively, after 6 hours of illumination. The rGO sample had a lower performance than the ZnO/rGO and Fe_2O_3/ZnO/rGO samples.

Recovery potential of materials after treatment with organic pigments

The recovery abilities of ZnO/rGO and Fe_2O_3/ZnO/rGO by a magnetic field after organic pigment treatment are shown in Figures 15 and 16.

Figure 15 shows that the recovery efficiencies of the ZnO/rGO material after 3 cycles are 68.2% and 61.2%, respectively. The efficiencies of treating MB and RhB after 3 cycles were 80.1% and 93.8%, respectively. Because the recovery efficiency was low, adding Fe_2O_3 to the material was necessary. The main role of Fe_2O_3 in the synthesized material is to improve photocatalytic recovery after dye treatment. In fact, recovery using a magnetic field is better than recovery using a filter. This is demonstrated by the recovery efficiencies of the Fe_2O_3/ZnO/rGO material after 3 cycles being 92.4% and 83.2%, respectively. The efficiencies of treating MB and RhB after 3 cycles were 81.3% and 94.7%, respectively. The addition of magnetic components leads to high magnetic recovery ability. Materials without magnetic components (Fe_2O_3) cannot be recovered by using a magnetic field. In addition, the reusability of Fe_2O_3/ZnO/rGO is high because the

decrease in photocatalytic activity to decompose pigments of the material is insignificant.

DISCUSSION

To prepare the Fe_2O_3/ZnO/rGO composite material, first, Fe_2O_3 and rGO were separately prepared. Figure 1 shows that all the functional groups in Fe_2O_3 were present in the typical absorption peaks of FT-IR. Similar absorption peak results were obtained by Bui et al.[8]. SEM images revealed that spherical Fe_2O_3 nanoparticles formed (Figure 2). The GO and rGO SEM images (Figures 3 and 4) show that GO is in the form of thick sheets, whereas rGO has stacked thin layers on top of each other, demonstrating that the process of peeling off the layer was performed during the reduction of GO to rGO by ascorbic acid[15]. The typical absorption peaks indicating the presence of oxygenated functional groups formed during the oxidation of graphite to GO (Figure 5) either dramatically decreased or disappeared in the FT-IR spectrum of rGO (Figure 6). This means that the oxygenated functional groups in GO were reduced by ascorbic acid during the formation of rGO. FT-IR and SEM analyses indicated that GO and rGO were successfully prepared and can be used for further steps. ZnO/rGO and Fe_2O_3/ZnO/rGO were then prepared via a hydrothermal method in which ZnO is formed in situ from ($Zn(CH_3COO)_2$ and doped on rGO sheets. SEM (Figures 7 and 8) revealed that the spherical ZnO and Fe_2O_3 nanoparticles were randomly dispersed on the surface of the graphene sheets. The low bandgap energy of Fe_2O_3/ZnO/rGO (Figure 12) facilitates the photocatalytic decomposition of dyes. The decrease
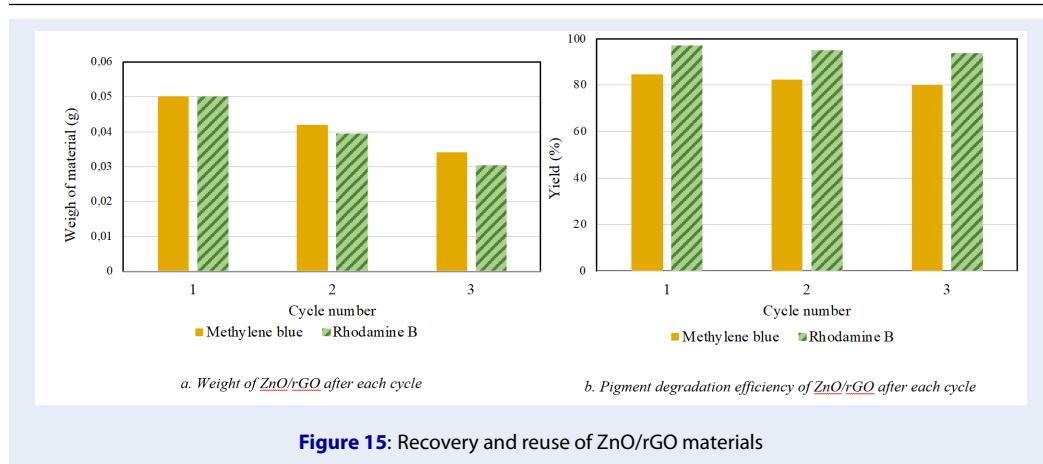
a. Weight of ZnO/rGO after each cycle

b. Pigment degradation efficiency of ZnO/rGO after each cycle

Figure 15: Recovery and reuse of ZnO/rGO materials

a. Weight of Fe₂O₃/ZnO/rGO after each cycle

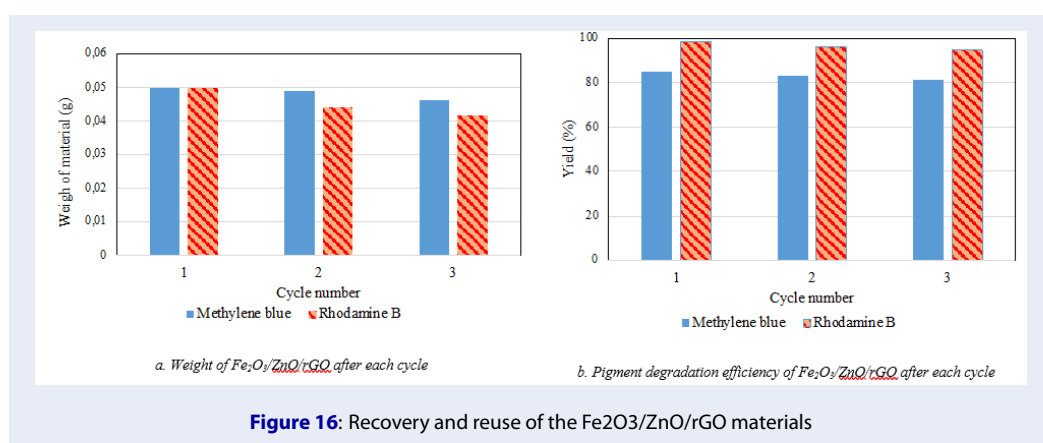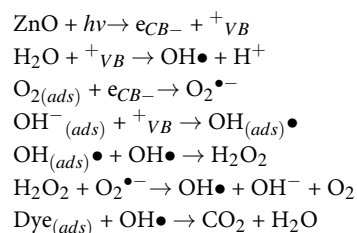b. Pigment degradation efficiency of Fe₂O₃/ZnO/rGO after each cycle

Figure 16: Recovery and reuse of the Fe2O3/ZnO/rGO materials

in the bandgap energy of the nanocomposite materials results in fast electron transfer and increased transition energy. The formation of Zn-O-C chemical bonds in the ZnO-rGO nanohybrid may be the reason for the decrease in the band gap energy. This also indicates that the electronic energy level of ZnO nanoparticles is affected by the presence of graphene in the material. More photons are easily absorbed, which improves the photocatalytic efficiency when the band gap energy is decreased [14,16].

The high-performance MB treatment (Figure 13) can be attributed to the adsorption of the rGO sample reaching its maximum capacity, proving that rGO is almost incapable of decomposing the MB pigment. Therefore, the main role of the rGO component in the MB treatment is adsorption. When ZnO/rGO and Fe$_2$O$_3$/ZnO/rGO were used, the MB concentration decreased to approximately 7 ppm, which corresponds to the photocatalytic decomposition of the MB pigment by the ZnO component. Like methylene blue, rhodamine B was treated with high yields by ZnO/rGO and Fe$_2$O$_3$/ZnO/rGO (Figure 14), whereas

rGO resulted in lower RhB treatment performance. These results indicate the role of ZnO in the high photocatalytic activity of materials.

The photodegradation mechanism of pigments is described below.

$$ZnO + hv \rightarrow e_{CB-} + {}^+{}_{VB}$$
$$H_2O + {}^+{}_{VB} \rightarrow OH\bullet + H^+$$
$$O_{2(ads)} + e_{CB-} \rightarrow O_2{}^{\bullet-}$$
$$OH^-{}_{(ads)} + {}^+{}_{VB} \rightarrow OH_{(ads)}\bullet$$
$$OH_{(ads)}\bullet + OH\bullet \rightarrow H_2O_2$$
$$H_2O_2 + O_2{}^{\bullet-} \rightarrow OH\bullet + OH^- + O_2$$
$$Dye_{(ads)} + OH\bullet \rightarrow CO_2 + H_2O$$

The improvement in the photocatalytic activity of the ZnO/rGO material can be attributed to the strong interaction between ZnO and rGO and the holes of graphene, which can act as good electron acceptors. When light was applied to the ZnO surface, electrons were excited from the valence band to the conduction band, leaving holes in the valence band. The transfer of these excited electrons from the conduction band of ZnO to the graphene sheet prolonged the recombination of electron–hole pairs, thereby promoting the

separation of the electron–hole pairs of ZnO [17,18]. The recovery potential of materials after the treatment of organic pigments is important because it shows the ability to apply materials on a large scale. Even though both ZnO/rGO and Fe_2O_3/ZnO/rGO lead to high MB and RhB treatments, only the Fe_2O_3/ZnO/rGO material can be highly recovered by a magnetic field, showing its advantages. Only a minor loss in Fe_2O_3/ZnO/rGO activity was observed (Figure 16) after three cycles, confirming the high potential of using Fe_2O_3/ZnO/rGO for treating organic pigments in wastewater.

CONCLUSION

Fe_2O_3, GO, rGO, ZnO/rGO and Fe_2O_3/ZnO/rGO materials were successfully prepared and characterized by SEM, FT-IR, and UV–Vis DRS. rGO can treat up to 55.1% MB and 71.4% RhB by adsorption, whereas ZnO/rGO and Fe_2O_3/ZnO/rGO can treat MB and RhB up to 84%-85% after 75 minutes and 97%-98% after 6 hours, respectively. The high conversion of MB and RhB in the presence of ZnO/rGO and Fe_2O_3/ZnO/rGO can be explained by photocatalytic degradation. The photocatalytic activity of the ZnO/rGO material may be due to the strong interaction between ZnO and rGO and the holes of graphene, which can act as good electron acceptors. The Fe_2O_3/ZnO/rGO material can be used for treating RhB MB and RhB with high efficiency and can be recovered and reused.

CONFLICT OF INTEREST

The authors agree that there are no conflicts of interest regarding the published results.

AUTHOR'S CONTRIBUTION

Nguyen Khac Duy, Uong Thi Ngoc Ha, Nguyen Van Thanh, and Pham Ngoc Anh performed the experiments, collected and processed the data and wrote the manuscript. Doan Thi Tram supports the processing of sequence data. Pham Van Tuan and Nguyen Thanh Tuan guided and planned the research. Bui Thi Le Thuy contributed to discussing the research results and completing the manuscript.

REFERENCES

1. Abdel Maksoud MIA, Elgarahy AM, Farrell C, Al-Muhtaseb AH, Rooney DW, Osman AI. Insight on water remediation application using magnetic nanomaterials and biosorbents. Coord Chem Rev. 2020;403;Available from: https://doi.org/10.1016/j.ccr.2019.213096.
2. Fonseca AFV, Siqueira RL, Landers R, Ferrari JL, Marana NL, Sambrano JR, Port FAL, Schiavon MA. A theoretical and experimental investigation of Eu-doped ZnO nanorods and its application on dye-sensitized solar cells. J Alloys Compd. 2018;739;Available from: https://doi.org/10.1016/j.jallcom.2017.12.262.
3. Iqbal T, Aziz A, Khan M, Andleeb S, Mahmood H, Khan AA, Khan R, Shafique M. Surfactant assisted synthesis of ZnO nanostructures using atmospheric pressure microplasma electrochemical process with antibacterial applications. Mater Sci Eng B. 2008;228:153-9;Available from: https://doi.org/10.1016/j.mseb.2017.11.027.
4. Rodwihok C, Wongratanaphisan D, Ngo YLT, Khandelwal M, Hur SH, Chung JS. Effect of GO additive in ZnO/rGO nanocomposites with enhanced photosensitivity and photocatalytic activity. Nanomaterials. 2019;9:1441;PMID: 31614525. Available from: https://doi.org/10.3390/nano9101441.
5. Kumar S, Kaushik RD, Upadhyay GK, Purohit LP. rGO-ZnO nanocomposites as efficient photocatalyst for degradation of 4-BP and DEP using high temperature refluxing method in in situ condition. J Hazard Mater. 2020;PMID: 33139108. Available from: https://doi.org/10.1016/j.jhazmat.2020.124300.
6. Xie J, Zhou Z, Lian Y, Hao Y, Li P, Wei Y. Synthesis of α-Fe2O3/ZnO composites for photocatalytic degradation of pentachlorophenol under UV-vis light irradiation. Ceram Int. 2015;41(2):2622-5;Available from: https://doi.org/10.1016/j.ceramint.2014.10.043.
7. Sujoy Kumar M, Kajari D, Saptarshi P, Sumit M, Avigyan N, Pabitra K, Bhattacharyaf TS, Achintya S, Rezaul S, Sukanta D, Debnarayan J. Engineering of ZnO/rGO nanocomposite photocatalyst toward rapid degradation of toxic dyes. Mater Chem Phys. 2019;223:456-65;Available from: https://doi.org/10.1016/j.matchemphys.2018.11.002.
8. Zhuang L, Haiyang F, Bo G, Yixuan W, Kui L, Yue S, Juntai Y, Jiawen K. In situ synthesis of Fe2O3/rGO using different hydrothermal methods as anode materials for lithium-ion batteries. Rev Adv Mater Sci. 2020;59:477-86;Available from: https://doi.org/10.1515/rams-2020-0046.
9. Sugianto S, Budi A, Endah FR, Triastuti S, Nabila Y, Irma FY, Didik A. Hydrothermal synthesis of GO/ZnO composites and their micromorphology and electrochemical performance. Int J Electrochem Sci. 2023;18(5):100109;Available from: https://doi.org/10.1016/j.ijoes.2023.100109.
10. Bui TTL, Pham NC, Pham TD, Nguyen LT. Preparation and characterization of graphene oxide based nanocomposite materials for solar energy sorption. Chem Pap. 2021;75(6):2425-40;Available from: https://doi.org/10.1007/s11696-020-01455-0.
11. Bùi Thị Lệ Thuỷ, Đào Đình Thuần, Phạm Đình Thảo. Using graphene oxide-based materials for thermal sorption. JST: Eng Technol Sustain Dev. 2021;1(1):21-7;Available from: https://doi.org/10.51316/jst.148.etsd.2021.31.1.5.
12. Hong RY, Fu HP, Di GQ, Zheng Y, Wei DG. Facile route to γ-Fe2O3/SiO2 nanocomposite used as a precursor of magnetic fluid. Mater Chem Phys. 2008;108(1):132-41;Available from: https://doi.org/10.1016/j.matchemphys.2007.09.014.
13. Andrijanto E, Shoelarta S, Subiyanto G, Rifki S. Facile synthesis of graphene from graphite using ascorbic acid as reducing agent. AIP Conf Proc. 2016;1725:020003;Available from: https://doi.org/10.1063/1.4945457.
14. Wen MYS, Abdullah AH, Ngee LH. Synthesis of ZnO/rGO nanohybrid for improved photocatalytic activity. Malays J Anal Sci. 2017;21(1):889-900;Available from: https://doi.org/10.17576/mjas-2017-2104-15.
15. Phan Thị Thùy Trang, Đỗ Thị Diễm Thúy, Nguyễn Thị Lan. Study structure properties of graphene oxide synthetic materials using ascorbic acid as reducing agent. J Anal Sci. 2022;27(3):125-9;.
16. Tewatia K, Sharma A, Kumar C. Synthesis of ZnO/rGO and green approach for its reduction by ascorbic acid. Proc Int Conf Front Sci Technol. 2021;2597:070006;Available from: https://doi.org/10.1063/5.0118780.
17. Yang Y, Liu T. Fabrication and characterization of graphene oxide/zinc oxide nanorods hybrid. Appl Surf Sci. 2011;257(21):8950-4;Available from: https://doi.org/10.1016/j.apsusc.2011.05.070.

18. Herring NP, Almahoudi SH, Olson CR, El-Shall MS. Enhanced photocatalytic activity of ZnO-graphene nanocomposites prepared by microwave synthesis. J Nanopart Res. 2012;14(12):1-13;Available from: https://doi.org/10.1007/s11051-012-1277-7.